

NUMERICAL INVESTIGATION OF THE LEAKAGE BEHAVIOUR OF REINFORCED CONCRETE WALLS

Christoph Niklasch*

Institut für Massivbau und Baustofftechnologie, Universität Karlsruhe (TH), Germany
Phone: +49 721 608 4352, Fax: +49 721 608 2265
E-mail: christoph.niklasch@ifmb.uni-karlsruhe.de

Laurent Coudert, Gregory Heinfling, Chantal Hervouet, Benoît Masson
EDF, France

Nico Herrmann, Lothar Stempniewski

Institut für Massivbau und Baustofftechnologie, Universität Karlsruhe (TH), Germany

Abstract

For the verification of nuclear power plant safety, the leakage behaviour of the containment walls is of decisive importance. In order to improve the knowledge of the leakage behaviour through cracks during a severe accident an experimental setup was developed at IfMB and several tests with different parameters were performed. To improve the understanding of the behaviour of the wall elements during the tests numerical simulations of the performed leakage experiments are necessary. Reliable numerical tools provide a basis for the transfer of the leakage behaviour from the tested specimens to the behaviour of whole containment structures. To address the task of developing tools for the numerical simulation of the leakage behaviour of reinforced containment structures, EDF and IfMB decided to cooperate. During this cooperation two different numerical approaches had been made basing on existing tools and models of EDF and IfMB. In the following sections a short overview about the two different models will be given. For the numerical investigation of the leakage phenomena IfMB used the commercial Finite-Element-Program ADINA with its capability to solve coupled fluid-structure-interaction (FSI) problems. EDF used two of their self-developed tools for the numerical simulation in a chained calculation: CODE ASTER® for the mechanical calculation of the specimen and ECREVISSE for the air/steam/water leakage flow calculation. The calculated leakage rates and temperature profiles of both models will be compared to the experimentally determined leakage rates and the results will be discussed.

Keywords: containment, leakage behaviour, numerical simulation

1 Introduction

During severe accidents in nuclear power plants high internal pressures accompanied by temperatures well over the water boiling temperature can occur and an air-steam mixture may be released through cracked containment walls.

Regarding the leakage of pure air through cracked concrete walls there are a couple of investigations introducing correlations based on crack width and pressure differential, like (Greiner & Ramm, 1995), or (Rizkalla et al., 1984). The leakage behaviour of water through cracked concrete walls has already been investigated as well by Edvardsen (1996) and Imhof-Zeitler (1993). Investigations on the leakage of steam and air through narrow, idealized cracks were performed in (Caroli et al., 1995).

To improve the knowledge about the leakage behaviour of reinforced concrete walls a test set-up was developed at the Institute of Reinforced Concrete Structures and Building Materials at the Universität Karlsruhe (TH). The results of the first series of tests were published by (Herrmann et al., 2002).

In this paper, numerical simulations of the test performed by IfMB and EDF will be presented and compared with the experimental results. More test results will be published by Stegemann (2005).

2 Numerical investigation performed by IfMB

For the simulation of the leakage behaviour of reinforced concrete walls, IfMB used a coupled fluid and structure calculation with the finite-element-program ADINA. Two separate models were used: A fluid model and a structural model.

2.1 Description of the Structural Model

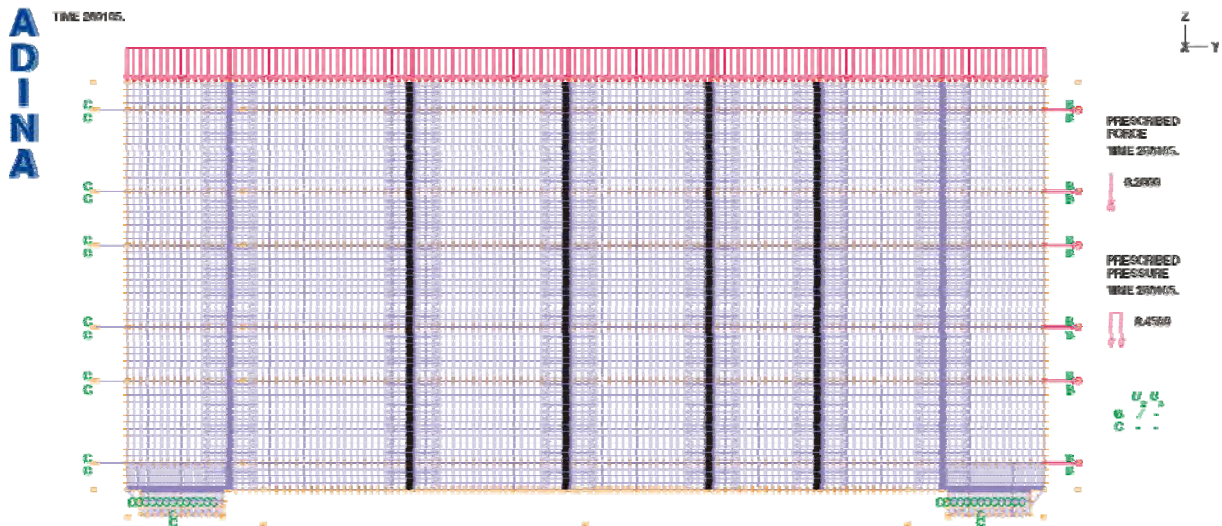


Fig. 1: Structural model

To define boundaries for the fluid-structure-interaction (FSI), discrete cracks were used for the structural model. Fig. 1 shows the structural model of the specimen. The concrete parts of the specimen were modelled with 4-node solid elements with a concrete material model developed at IfMB. For the modelling of the reinforcement, 2-node truss elements were used. The beam elements were connected to the solid elements with 4-node bond elements with an embedded bond model.

According to the experimental set-up the left ends of the reinforcement bars were connected to spring elements. The stiffness of the spring elements was similar to the stiffness of the reinforcement bars with a diameter of 63 mm which were each connected to 4 reinforcement bars lying inside the specimen. The other end of the spring elements was fixed equivalent to the anchorage of the reinforcement bars at the left side of the experimental set-up.

At the right end of the reinforcement bars a force load was applied with the same force on every reinforcement bar as in the experimental set-up. Fig. 1 shows the structural model with the applied boundary conditions and loads.

The five inner cracks were equipped with FSI-boundary conditions to allow the interaction with the fluid model. With an iterative calculation the displacements and stresses at these boundaries were coupled between the two models.

2.1.1 Bond elements

There are many different approaches to transfer forces between concrete and reinforcement elements (Akkermann, 2000). In (Keuser, 1985) and (Mainz, 1993) overviews on the different bond element formulations are given. The used formulation of a linear bond element is based on the work of Keuser (1985) and was implemented in ABAQUS by Akkermann (2000). For the calculation of the leakage behaviour it was ported to ADINA.

As element type 4-node isoparametric elements with a linear displacement assumption had been chosen for the implementation of the bond element. In the unloaded state the bond element has only one dimension. It consists of two pairs of nodes. Each pair itself consists of one reinforcement node and one concrete node with

the same original position. With nodal displacements the bond element is becoming two-dimensional. Since the nodal displacements are very small compared to the original length of the element, only the line of symmetry between the two node-pairs is considered. This symmetric line is called contact line (see Fig. 2).

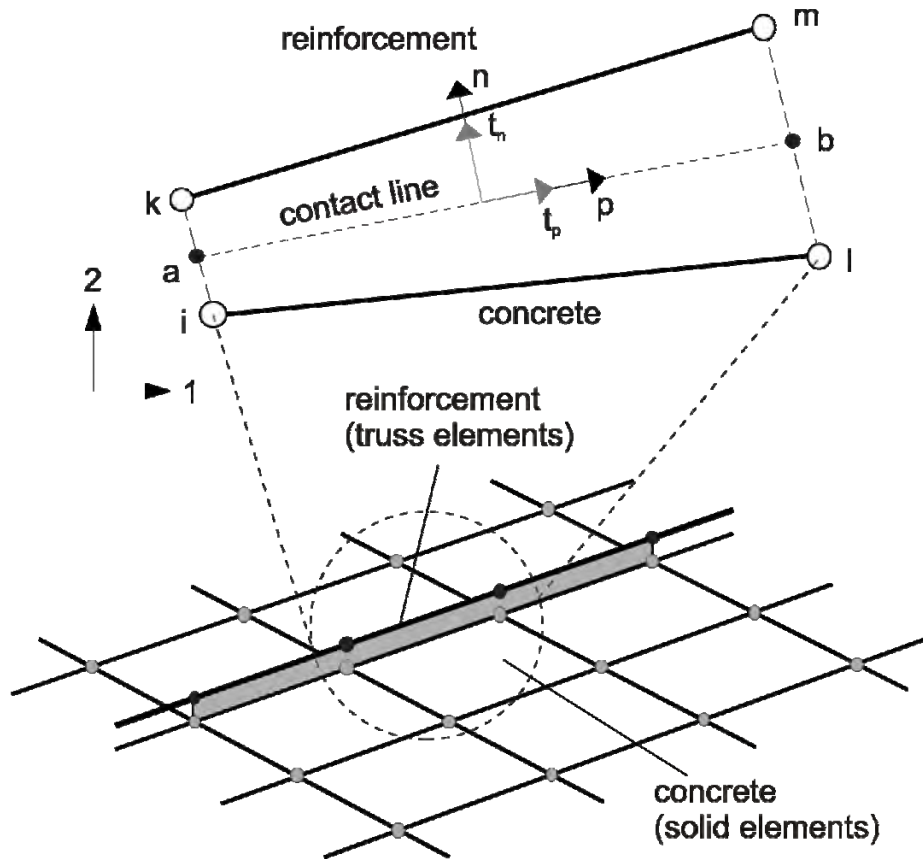


Fig. 2: Linear bond element, according to Keuser (1985)

Starting with the global node displacements u of the attached reinforcement and concrete nodes and the help of form functions the local parallel and transversal relative displacements at the contact line were calculated.

$$\underline{\delta}(p) = \tilde{T} \cdot \underline{B} \cdot u$$

with

$$\tilde{T} = \text{transformation matrix from global to local coordinate system}$$

$$\underline{B} = \text{matrix of the form functions}$$
(2.1)

The stresses $\underline{\tau}(p)$ at the contact line are then calculated with the local relative slip $\underline{\delta}(p)$ at the contact line and a bond model. The used bond model is based on the work of (den Uijl & Bigaj, 1996).

$$\underline{\tau}(p) = \underline{E} \cdot \underline{\delta}(p)$$
(2.2)

The component of $\underline{\tau}(p)$ which is parallel to the reinforcement axis is the bond stress of the bond models. The stress component perpendicular to the reinforcement axis is the resistance against lateral pressure. With the stresses and the material stiffness matrix, the nodal force vector and the element stiffness matrix can be calculated (Akkermann, 2000).

$$\underline{f}_{el} = \frac{l_{el}}{2} \int_{-1}^1 \underline{B}^T (\tilde{T}^T \underline{A}_b \underline{\tau}) dp$$
(2.3)

$$\underline{K}_{el} = \frac{l_{el}}{2} \int_{-1}^1 \underline{B}^T (\tilde{\underline{T}}^T \underline{A}_b \underline{E}_b \tilde{\underline{T}}) dp$$

(2.4)

with

l_{el} = element length

\underline{A}_b = contact layer matrix

2.1.2 Concrete

In this section a short overview on the used concrete material model is given. For details, see (Akkermann, 2000).

Concrete is a material with an inhomogeneous structure consisting of coarse aggregates and a continuous matrix, which itself comprises a mixture of cement paste and smaller sand particles (Chen, 1994). Concrete has a highly nonlinear behaviour under mechanical loadings, largely determined by the internal structure of the composite. The deformation behaviour as well as the strength depends on the type of loading. The microscopic material behaviour is determined by a combination of many physical and chemical material laws and implicates many local effects. However, for most of the calculations the global behaviour of the structure is of interest. Macroscopic material models are more suitable for this kind of tasks and the material behaviour is homogenised for this type of material models.

In the implemented material model, a macroscopic damage evolution model (Lemaitre, 1992) is used. In this model, the change of the stiffness of the damaged material depends on the irreversible damage value D :

$$\sigma = (1 - D)E_{c0}\varepsilon \quad (2.5)$$

$$D = \text{damage value; } 0 \leq D \leq 1 \quad (2.6)$$

$$E_{c0} = \text{original stiffness} \quad (2.7)$$

The change of the damage value D depends on the load evolution. Since the damage is defined as irreversible, D has to be always positive: $D \geq 0$. For this reason, the secant stiffness $E^{t:cs}$ is used, if the material is unloaded.

$$E_{cs}^t = (1 - D)E_{c0} \quad (2.8)$$

Plastic deformations and time-dependent effects are not considered in the material model that was used.

2.2 Fluid Model

The fluid model for the coupled FSI-calculation is shown in Fig. 3.

For the fluid model the following main assumptions have been made:

- Time dependent temperature load on the top surface (pressure chamber)
- Radiation and convection boundaries with a constant environment temperature at the bottom surface
- Constant conductivity and heat capacity of the concrete
- Laminar flow
- Two-Phase flow with the same velocities for the two phases (homogeneous equilibrium model)

The calculated temperatures and stresses at the fluid-structure boundaries of the fluid model were then used as an input parameter for the structural model. The structural model calculates the displacement of the specimen and modifies the fluid-structure boundary of the fluid model for the next iteration step. Table 1 summarises the used material and boundary condition parameters.

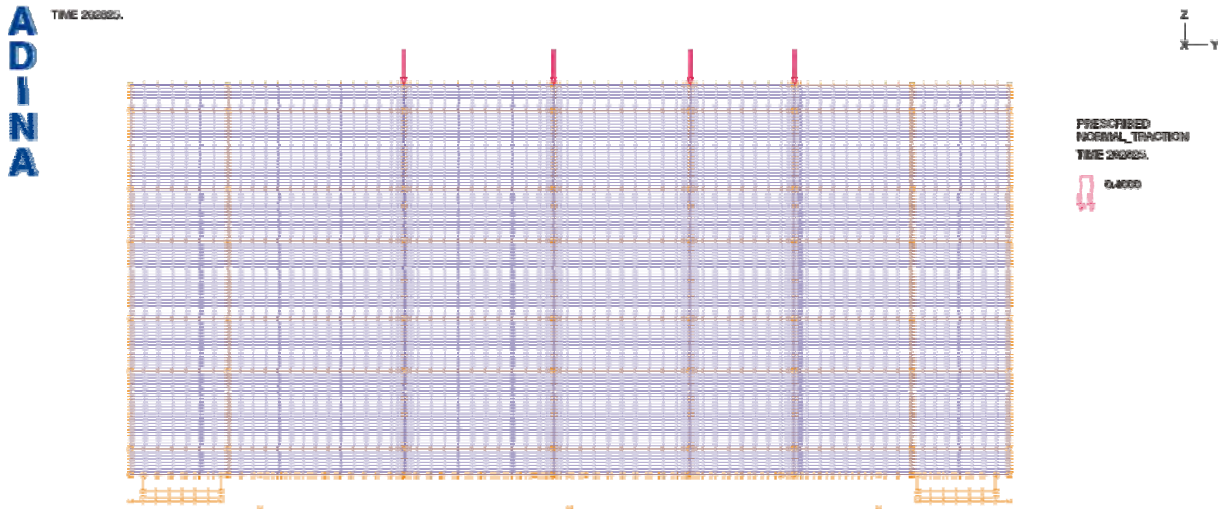


Fig. 3: Fluid model

		<i>Table 1: Parameters for the thermal model</i>	
Concrete:	Thermal Conductivity	$\lambda = 2.3 \frac{\text{kg} \cdot \text{m}}{\text{s}^3 \cdot \text{K}}$	
	Specific Heat Capacity	$c_p = 1250 \frac{\text{m}^2}{\text{s}^2 \cdot \text{K}}$	
Convection	Convection Coefficient	$H = 8 \frac{\text{W}}{\text{m}^2 \cdot \text{K}}$	

2.2.1 Description of the used Laminar Fluid Model

The used Finite Element program ADINA has the possibility to calculate coupled fluid-structure problems. Compared to specialised Computational Fluid Dynamics (CFD) programs like FLUENT, FIDAP, STAR-CD or CFX the capabilities in the fluid part are not as sophisticated as in the specialised CFD programs. On the other hand it is not possible to describe the structural aspects adequately with the CFD programs.

For the description of multiphase fluid flows different models had been developed for example the homogeneous flow model, the separated flow model and the two fluid model (Johnson, 1998). Unfortunately ADINA contains no two-phase or multi-phase flow models. Therefore the Homogeneous Equilibrium Model (HEM) is the only possibility to describe the flow conditions inside the cracks of the specimen.

2.2.2 Homogeneous Equilibrium Model

In the homogeneous equilibrium model it is assumed that the velocity, temperature and pressure between the phases or components are equal. This is based on the assumption that differences in these three potential variables will cause momentum, energy and mass transfer between the phases rapidly enough so that equilibrium is reached (Johnson, 1998).

For flows with one phase finely dispersed in another phase like bubbly flow of air in water or steam in water at high pressures this assumption can be made.

The thermodynamic properties of a two-phase flow modelled with the HEM are functions of the volume fractions α_i and the mass fractions X_i of the phase i .

$$\text{Mixture density} \quad \rho = \sum \alpha_i \cdot \rho_i \quad (2.9)$$

$$\text{Internal energy} \quad u = \sum X_i u_i \quad (2.10)$$

$$\text{Specific volume} \quad v = \sum X_i \cdot v_i = \frac{1}{\rho} \quad (2.11)$$

The multiphase transport properties of viscosity μ and thermal conductivity k are problematic too, because it is difficult to decide how one should average their effect: in an area average, mass average or volume average sense. For many situations the mixture transport properties have been arbitrarily averaged on a volume average or mass average basis (Johnson, 1998):

$$\mu = \sum \alpha_i \cdot \mu_i \quad (2.12)$$

or

$$\mu = \sum X_i \cdot \mu_i \quad (2.13)$$

Sometimes especially if one phase is dominant like liquid in a channel with low amount of gas the multiphase effects are neglected and the liquid or gas properties of viscosity and thermal conductivity are used.

In our implementation of the homogeneous equilibrium model, the mass average is used for the viscosity, the specific heat and the thermal conductivity of the mixture.

2.2.3 Steam Properties

For the pressure and temperature dependent properties of the steam phase the IAPWS-IF97 formulation is used (Wagner et al., 1997), (Wagner, 1998).

The IAPWS Industrial Formulation covers the following range:

$$\begin{array}{ll} 273.15 \text{ K} \leq T \leq 1073.15 \text{ K} & \text{for } p \leq 100 \text{ MPa} \\ 1073.15 \text{ K} \leq T \leq 2273.15 \text{ K} & \text{for } p \leq 10 \text{ MPa} \end{array}$$

2.3 Comparison between Calculation and Measurement

For the simulation of the first test with the third specimen of the test series (Stegemann, 2004), the temperature was applied with a convection boundary condition at the top surface of the specimen. The conductivity and heat capacity of the concrete was assumed to be temperature dependent. The measured remaining crack width of 0.7 mm of the previously opened cracks was taken into account.

The fluid is only flowing through the four cracks inside the observation area. The temperature distribution at the end of the calculated steam test (Fig. 4) shows the influence of the fluid flowing through the cracks on the temperature of the surrounding concrete. Due to the thermal strain of the concrete the displacement and deformation of the specimen is influenced, too.

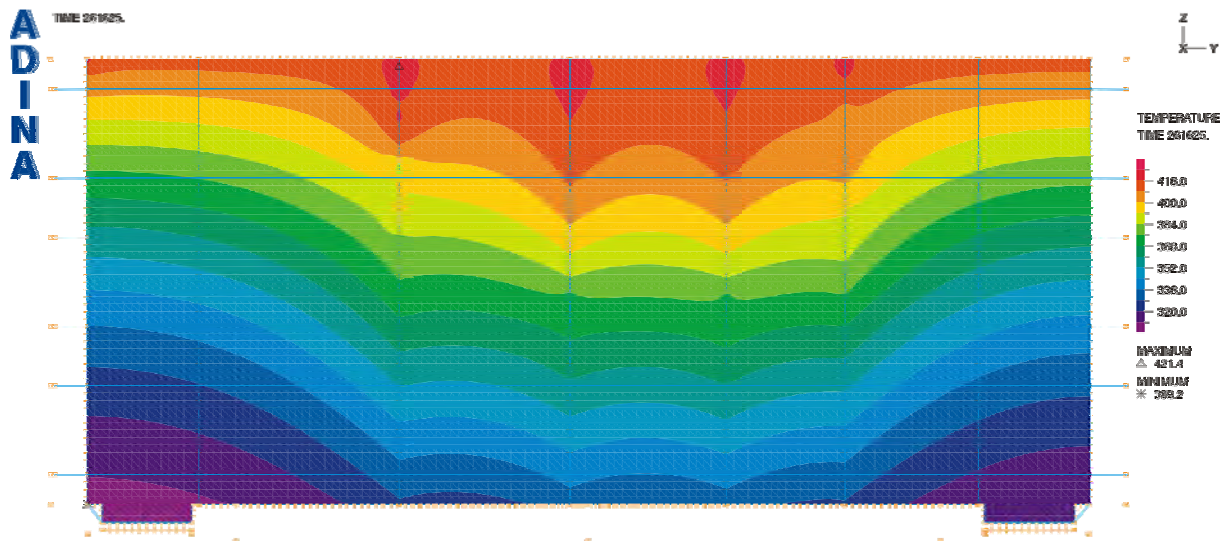


Fig. 4: Temperature distribution after 72 h

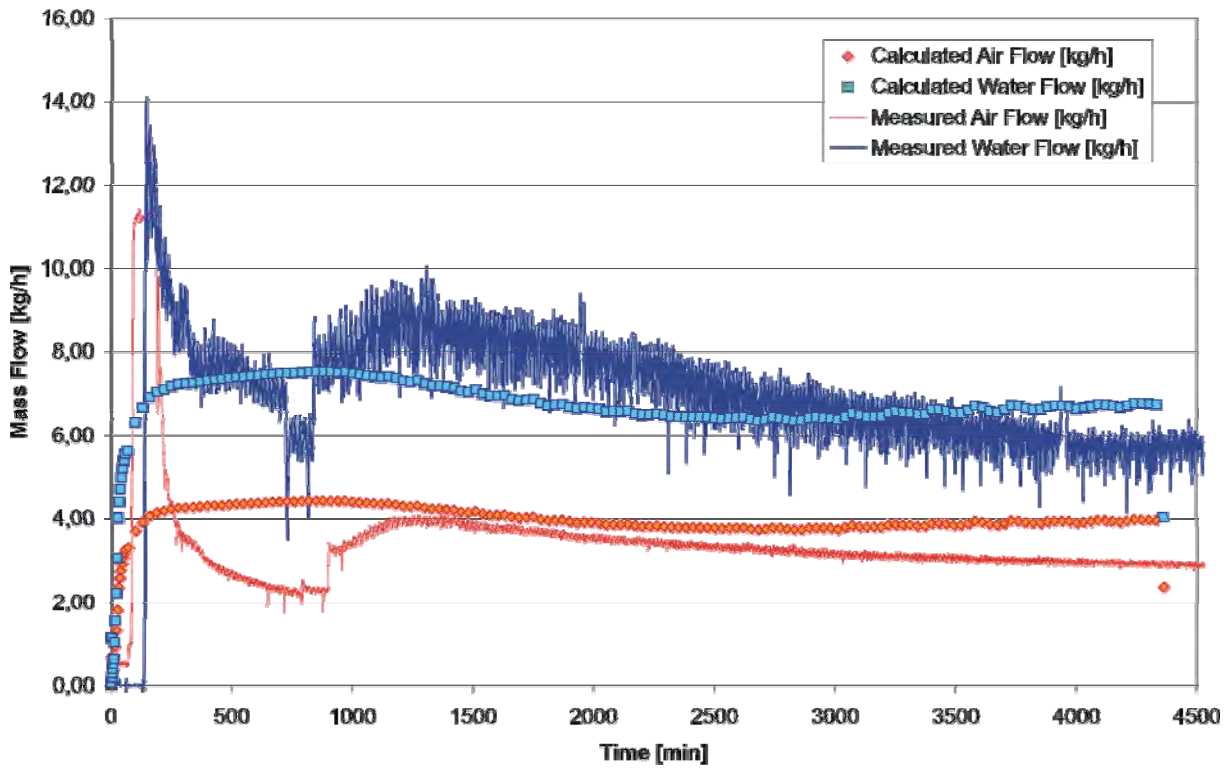


Fig. 5: Comparison between measured and calculated leakage flow

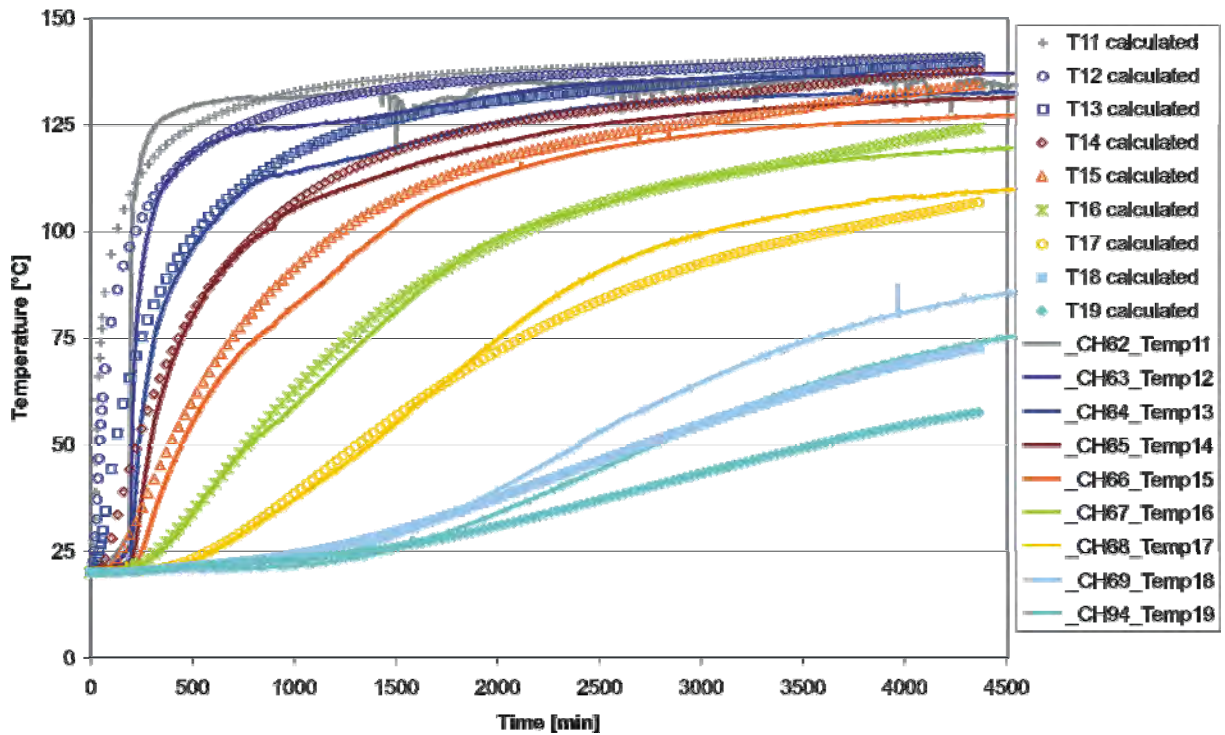


Fig. 6: Comparison between measured and calculated temperatures

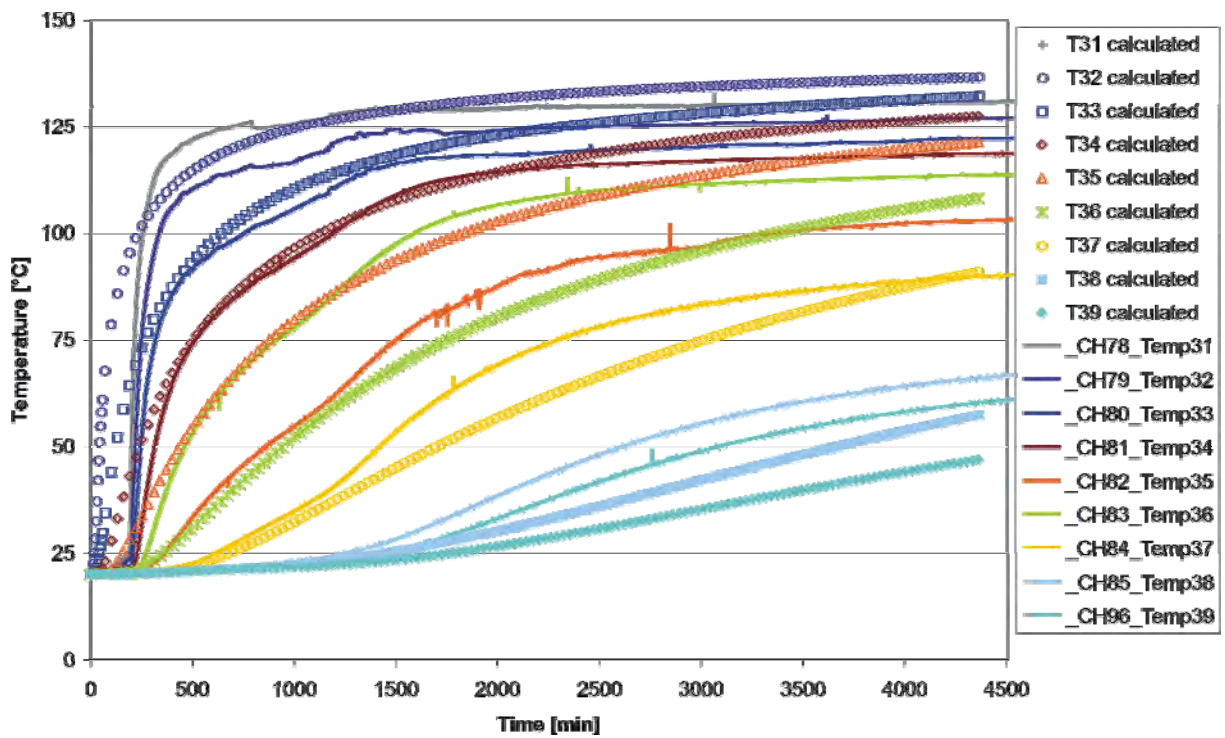


Fig. 7: Comparison between measured and calculated temperatures

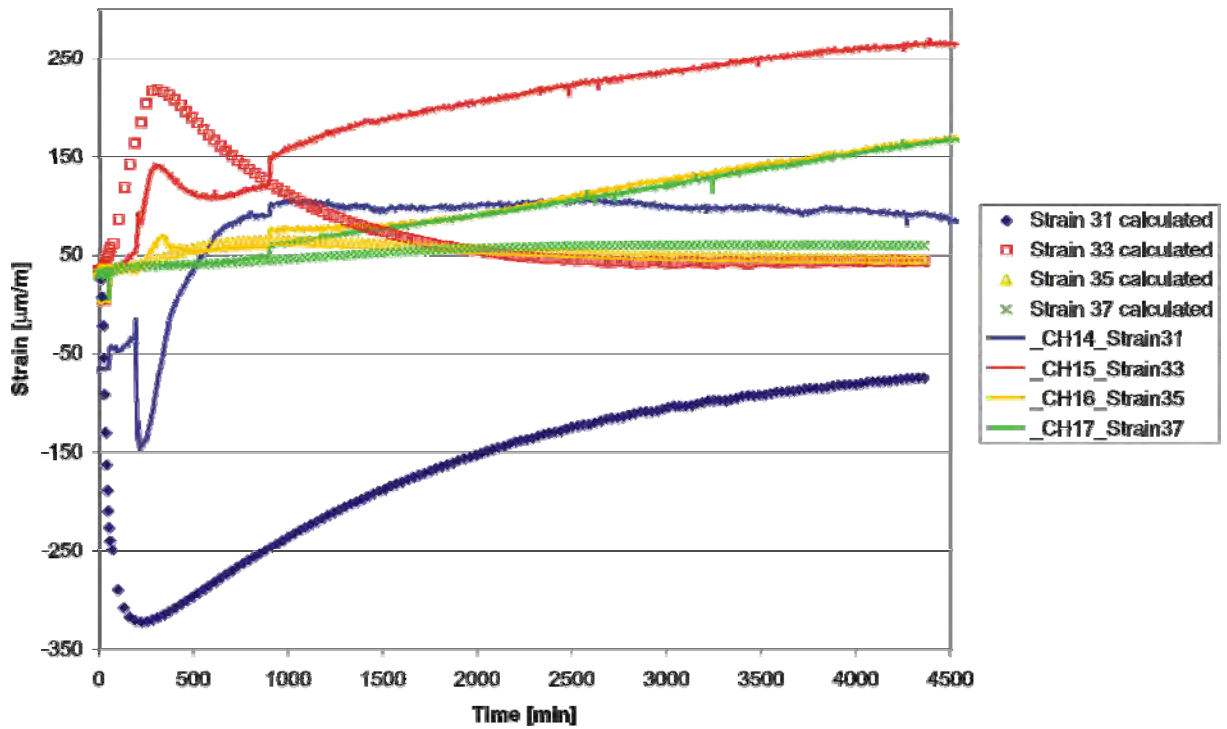


Fig. 8: Comparison between measured and calculated strains

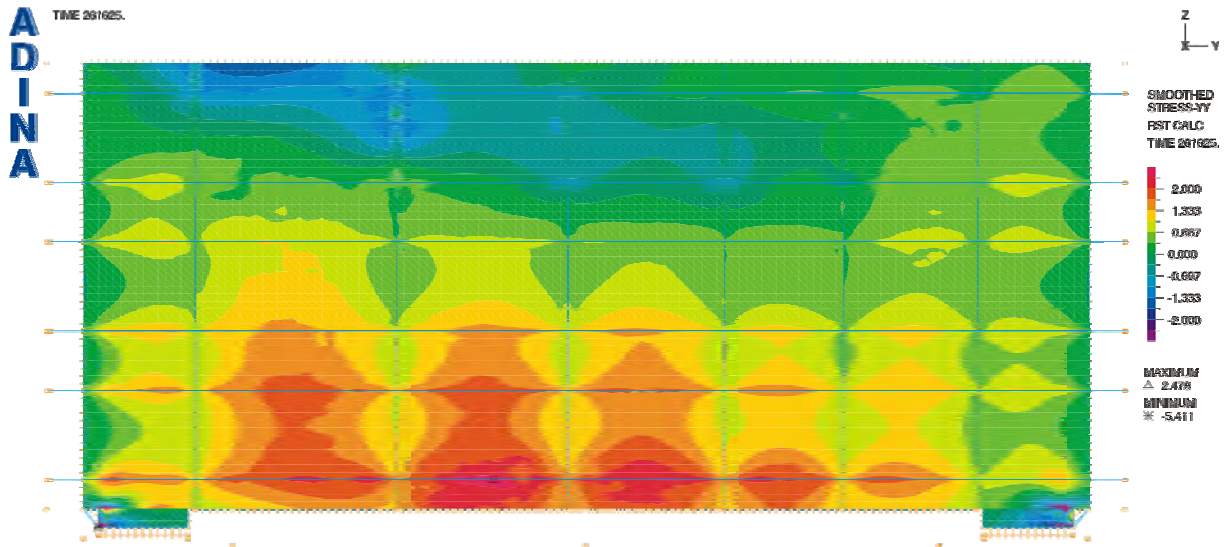


Fig. 9: Concrete stresses in longitudinal direction after 72 h

3 Numerical investigation performed by EDF

The EDF calculation is performed with CODE ASTER® for the thermo mechanics calculations and with ECREVISSE for fluid calculations.

3.1 Principle of the 3D model

One quarter of the slab (symmetry along the main axis, the thickness being conserved to scale 1:1) is represented (length (y): 1.35 m, width (x): 0.90 m, depth (z): 1.20 m). The concrete is modelled with cubic elements. The rebars (length: 1.8 m) are modelled with 1D beam elements. Three discrete cracks are represented, among which two are located in the observation area.

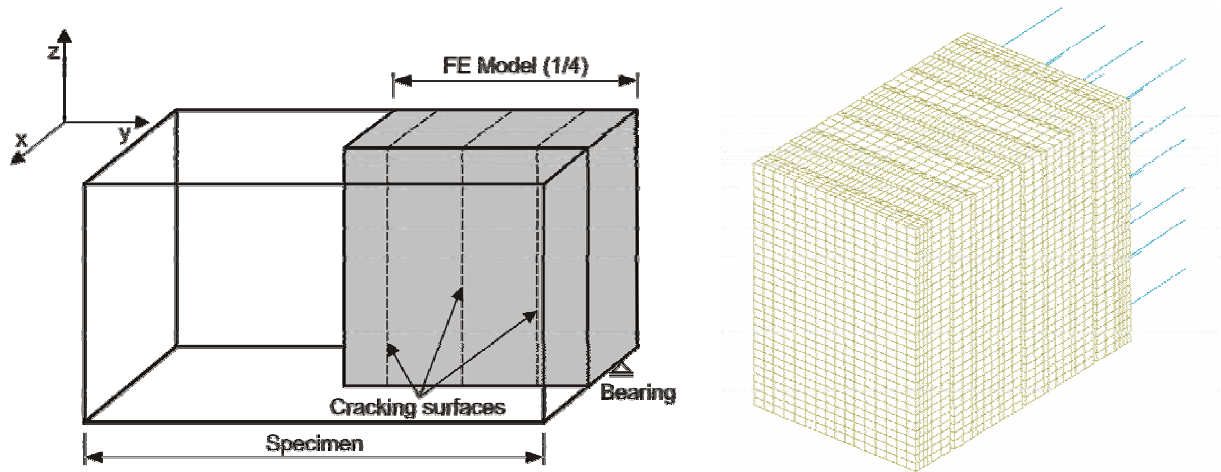


Fig. 10: Discrete crack model

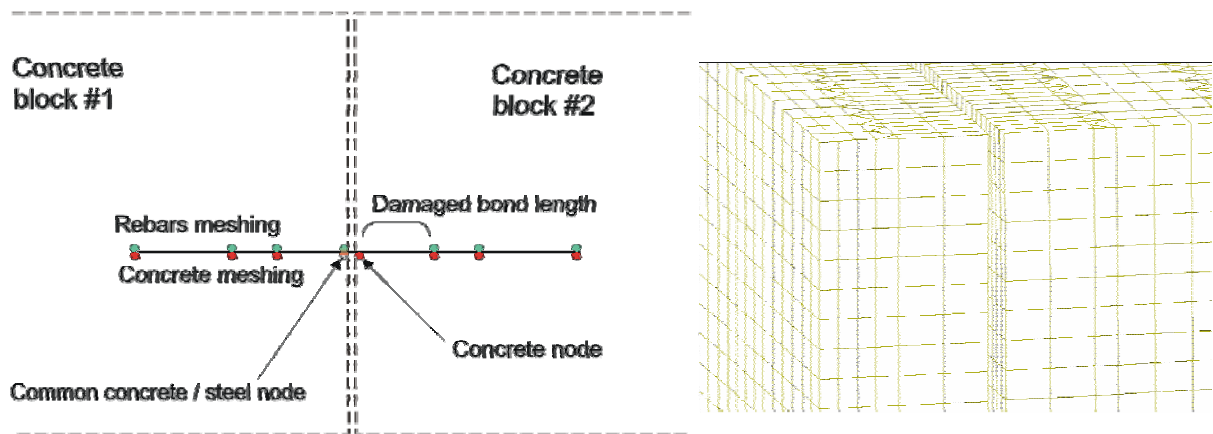


Fig. 11: Detail of the discrete crack model

- Among the two concrete nodes located at the crack surface, one belongs to the rebars.
 - The crack profile is strongly dependent on the damaged bond length which is simulated by the length of the last rebar element near the crack.
 - The vertical displacement of concrete nodes on each block near the rebars must be the same.
- The force applied by the hydraulic jacks is taken into account as a displacement at the ends of the rebars.

3.2 Temperature calculation

The temperature is applied at the top surface with a time dependent convection coefficient: $4 \frac{W}{m^2 \cdot K}$ for the first two hours with a linear increase up to $75 \frac{W}{m^2 \cdot K}$ during the two following hours. The thermal conductivity is $2.3 \frac{W}{m \cdot K}$ and the specific heat capacity is $1240 \frac{J}{kg \cdot K}$.

The calculated temperature values are higher than the experimental results close to the top surface (see Fig. 12). In the levels between 25 cm and 60 cm below the top surface, experimental temperatures are significantly higher than the calculated ones.

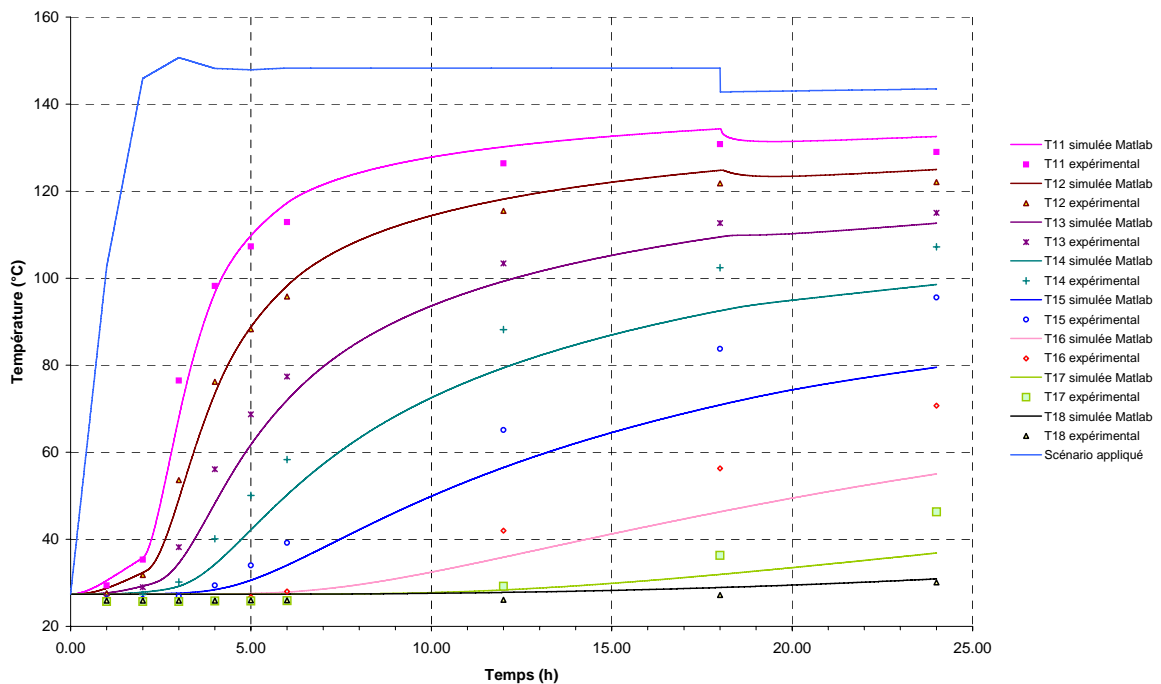


Fig. 12: Comparison between measured and calculated temperatures

3.3 Thermo mechanics and leakage calculations

3.3.1 Air test

For the calculation, the dead load of the slab, the temperature and the pressure at the top surface are taken into account in order to know the crack profile for the fluid calculation with ECREVISSE.

The first simulation is one of an air test : CODE ASTER® gives crack profiles which are used as input data for leakage calculations with ECREVISSE. Additional required input data is: air, steam and water ratio, pressure and temperature at the top surface. ECREVISSE provides leakage rates and air, steam and water ratio at the bottom surface. As friction and roughness coefficients are adjusted, the model gives good agreement with the experimental results. The main conclusion of the numerical simulation of the air test turns out to be that the best way to represent a closed crack is to model it as an opened crack whose crack width varies from $20 \mu m$ to $50 \mu m$. For further air/steam calculations with closed cracks, a value of $40 \mu m$ for crack width has been chosen.

3.3.2 Steam test

Crack widths calculated are displayed in Fig. 13. For the leakage calculation, the minimum crack width is $40 \mu m$, as explained before.

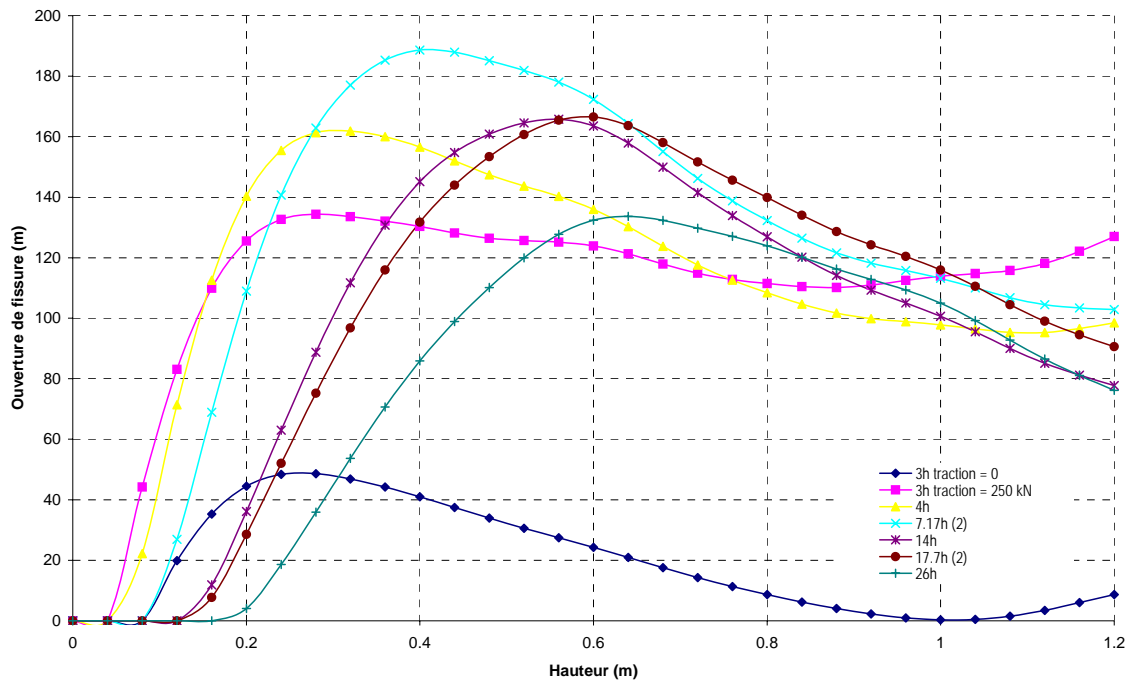


Fig. 13: Crack width profiles for several time steps in the width slab

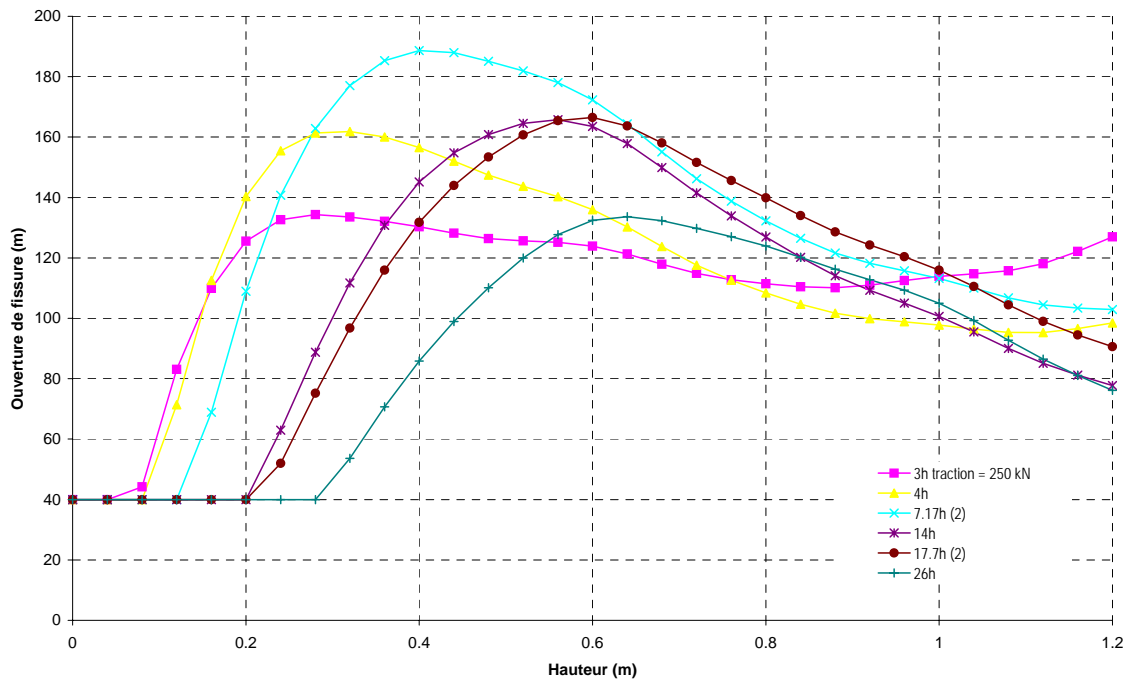


Fig. 14: Crack width profiles for leakage calculation (entry data)

The calculated crack profiles with a minimum crack width of $40 \mu\text{m}$ (see Fig. 14) and calculated temperatures are used as input data for ECREVISSE calculations (1D). The hypotheses for ECREVISSE calculations are that the flow is stationary and the fluid is homogeneous in the perpendicular flow plan. Phase change can occur along the crack: water can vaporise or steam can condense.

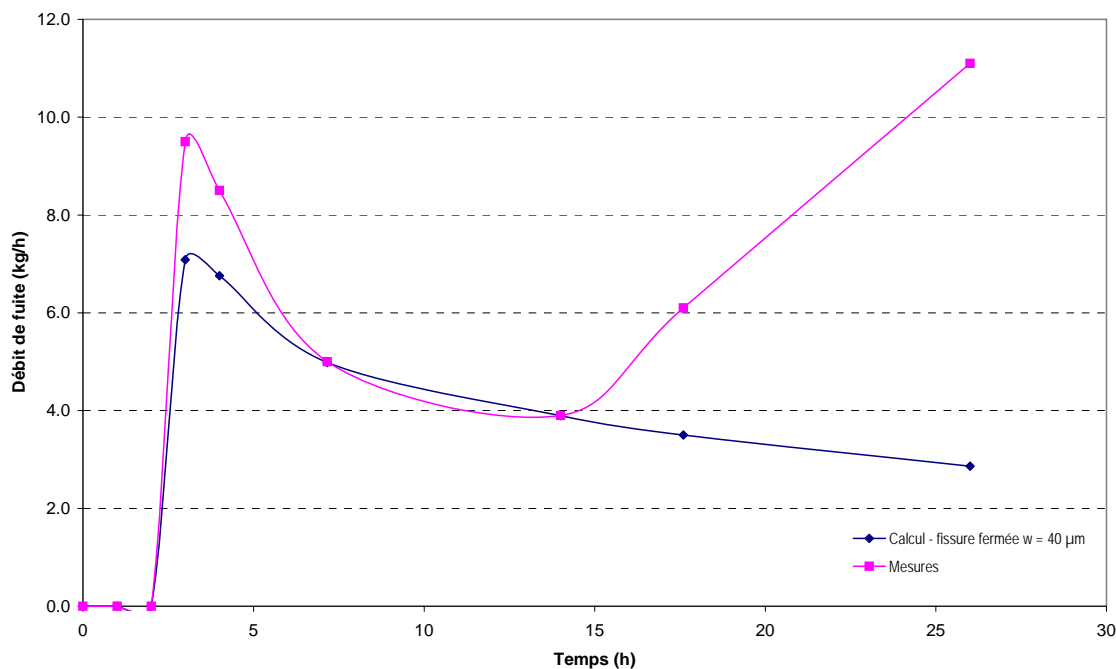


Fig. 15: Comparison between leakage calculation and experimental results

There is a good agreement between simulation results and experimental measurements until 14 hours. After 14 hours, the simulation result slightly decreases although the measurement increases again. The difference is due to the calculated temperatures which are different from the measured ones. But in our model, the temperature dependent dilatation closes the crack and as a result the leakage is reduced.

Other calculations will be performed with the following improvements:

- take into account the fluid structure interaction (effect of fluid pressure and fluid induced heating of the crack walls).
- take into account the fluid pressure in the crack which could widen the crack openings

4 Conclusions

Due to the used homogeneous equilibrium model for the calculations of IfMB the velocities of the fluid phases are equal and the mass ratio of the phases remain constant. Therefore the mass ratio at the crack outlet is determined by the mass ratio at the inlet.

The calculated leakage flow through the four cracks inside the observation area fits the measured leakage flow quite good and is mainly influenced by the remaining crack width and the mass ratios of the tested air-steam mixture.

The model of EDF shows a good agreement between the calculation and the measurement for the leakage flow in the first hours. It should be improved within the future work by taking into account the fluid structure interaction.

So far, it has not been considered to model the flow through porous media along the crack in both models.

More investigations should be performed on the temperature behaviour of the specimen due to the following deficiencies:

- In the upper part the calculated temperatures of both models are too high compared to the measured ones especially in the middle of the specimen between the two cracks with the smallest distance. In the IfMB model the concrete is heated too much from the fluid flow inside the cracks.
- In the lower part of the specimen the temperatures are underestimated compared to the measurements.

IfMB and EDF are planning to simulate all tests on all specimens.

5 References

- Akkermann, Jan. 2000. Rotationsverhalten von Stahlbeton-Rahmenecken. Ph.D. thesis, Institut für Massivbau und Baustofftechnologie, Universität Karlsruhe (TH).
- Caroli, C., Coulon, N., Morton, Williams. 1995. Theoretical and experimental investigations on the leakage of steam, gas and aerosols through narrow cracks and capillaries. In: Symposium on EU Research on Severe Accident, Luxembourg.
- Chen, Wai-Fah. 1994. Constitutive Equations for Engineering Materials. Elsevier Science B.V.
- den Uijl, Joop A., Bigaj, Agnieszka J. 1996. A bond model for ribbed bars based on concrete confinement. *Heron*, **41**(3), 199–226.
- Edwardsen, Carola Katharina. 1996. Wasserdurchlässigkeit und Selbstheilung von Trennrissen in Beton. DAfStb 455, Rheinisch-Westfälische Technische Hochschule Aachen.
- Greiner, U., Ramm, W. 1995. Air leakage characteristics in cracked concrete. *Nuclear Engineering and Design*, **156**(1-2), 167–172.
- Herrmann, Nico, Niklasch, Christoph, Stegemann, Michael, Stempniewski, Lothar. 2002 (Apr.). Investigation of the leakage behaviour of reinforced concrete walls. In: The Evaluation of Defects, Repair Criteria & Methods of Repair for Concrete Structures on Nuclear Power Plants. OECD Nuclear Energy Agency.
- Imhof-Zeitler, Christiane. 1993. Fließverhalten von Flüssigkeiten in durchgehend gerissenen Betonkonstruktionen. DAfStb 460.1, Institut für Massivbau, TH Darmstadt.
- Johnson, Richard W. (ed). 1998. The Handbook of Fluid Dynamics. CRC Press.
- Keuser, Manfred. 1985. Verbundmodelle für nichtlineare Finite-Elemente-Berechnungen von Stahlbetonkonstruktionen. VDI-Verlag.
- Lemaitre, J. 1992. A Course on Damage Mechanics. Springer.
- Mainz, Jürgen. 1993. Modellierung des Verbundtragverhaltens von Betonrippenstahl. Ph.D. thesis, Technische Universität München.
- Rizkalla, Sami H., Lau, Bon L., Simmonds, Sidney H. 1984. Air leakage characteristics in reinforced concrete. *Journal of Structural Engineering*, **110**(5), 1149–1162.
- Stegemann, Michael. 2005. Experimentelle Untersuchungen zur Leckage von Luft- und Dampfgemischen durch gerissene Stahlbetonwände. to be published in 2005.
- Wagner, W., Cooper, J. R., Dittmann, A., Kijima, J., Kretzschmar, H.-J., Kruse, A., Mares, R., Oguchi, K., Sato, H., Stöcker, I., Sifner, O., Takaishi, Y., Tanishita, I., Trübenbach, J., Willkommen, Th. 1997. Release on the IAPWS Industrial Formulation 1997 for the Thermodynamic Properties of Water and Steam. The International Association for the Properties of Water and Steam.
- Wagner, Wolfgang. 1998. Properties of Water and Steam: The Industrial Standard IAPWS-IF97 for the Thermodynamic Properties and Supplementary Equations for other Properties. Springer-Verlag.